Diamond & Related Materials 127 (2022) 109124

Contents lists available at ScienceDirect

Diamond & Related Materials

journal homepage: www.elsevier.com/locate/diamond

Effect of ionic strength on amorphous carbon during chemical mechanical planarization

Seungjun Oh [a,1], Cheolmin Shin [a,1], Donggeon Kwak [a], Eungchul Kim [a], Juhwan Kim [a], Chulwoo Bae [b], Taesung Kim [a,b,*]

[a] School of Mechanical Engineering, Sungkyunkwan University, Suwon, Republic of Korea
[b] SKKU Advanced Institute of Nanotechnology (SAINT), Sungkyunkwan University, Suwon, Republic of Korea

ARTICLE INFO

Keywords:
Amorphous carbon
CMP
Chemical reaction

ABSTRACT

A hard mask is an essential to prevent pattern collapse resulting from leaning, wiggling, or other defects. It is critical to achieve high removal rates of hard masks. The process of amorphous carbon chemical mechanical planarization (CMP) forms OH radicals on the surface by an oxidation and breaks bonds in the weakest area. Electrolytes with different ionic strengths were added, to facilitate the formation of OH radicals. When electrolytes were added, the removal rates increased by approximately 2.3 times over those without any additives. The increase in surface roughness is another significant factor. The roughness increased in all cases. In particular, a mixed slurry achieved the best results, with a mean surface roughness value of 0.147 nm for a scanning area of $5 \times 5\ \mu m^2$. Thus, the ionic strength of the electrolyte is critical in the CMP of amorphous carbon.

1. Introduction

As the feature sizes shrink to the sub-10 nm scale in the semiconductor industry, high aspect ratios are required to realize high stacking technologies. However, in the lithography process, problems such as leaning, wiggling, and other defects may occur. A hard mask is an advantageous structure that can prevent collapse by increasing the aspect ratio [1]. Amorphous carbon is one of the most widely used materials for hard masks. Amorphous carbon, a diamond-like carbon, exhibits complex properties due to the presence of sp^2 and sp^3 orbitals. Of these, properties such as hardness and chemical resistance result from the sp^3 orbitals, whereas the low surface fricative force results from the sp^2 orbitals [2]. The sp^2 orbital is not a weaker bond than the sp^3 orbital; however, the bond formed by a layer of sp^2 orbitals results in a weaker van der Waals bond than that of the sp^3 orbitals. These characteristics can be altered by optimizing the concentration [3]. Several deposition methods have been investigated for the controlled growth of amorphous carbon films [4]. These methods include chemical vapor deposition, ion-beam deposition, and laser deposition [3]. Owing to its amorphous nature, the carbon structure is hard, and the surface exhibits high roughness. Therefore, chemical mechanical planarization (CMP) is required to achieve global planarization. CMP is an important process in the semiconductor industry which involves a combination of chemical reactions and mechanical abrasion, with various components, such as polishing pads, conditioners, and slurries.

Polishing amorphous carbon is a challenging process owing to its unique properties. Taking into account the variety of properties needed and processes involved, we selected commercial colloidal silica as the abrasive and set up the mechanical conditions to induce oxidation. Silica is widely used to develop CMP slurries to polish metals and alloys such as copper, sapphire, titanium, nickel alloys, and diamond [5–8]. High-performance surfaces were fabricated using the developed slurries for application in the semiconductor and microelectronics industries [9]. The commonly used hydrogen peroxide was selected as the oxidant owing to its efficiency [10]. To aid oxidation, we introduced electrolyte additives to obtain an electrically conductive solution upon dissolution in a solvent [11–15].

This paper reports, the CMP process carried out using colloidal silica and polyurethane hard polishing pads. The removal rates and flatness of the surface were improved by the slurry containing oxidants and electrolytes. In addition, chemical bonding analysis confirmed the removal mechanism of the amorphous carbon layer.

* Corresponding author at: School of Mechanical Engineering, Sungkyunkwan University, Suwon, Republic of Korea.
E-mail address: tkim@skku.edu (T. Kim).
[1] These authors contributed equally to this work.

https://doi.org/10.1016/j.diamond.2022.109124
Received 27 January 2022; Received in revised form 17 May 2022; Accepted 18 May 2022
Available online 25 May 2022

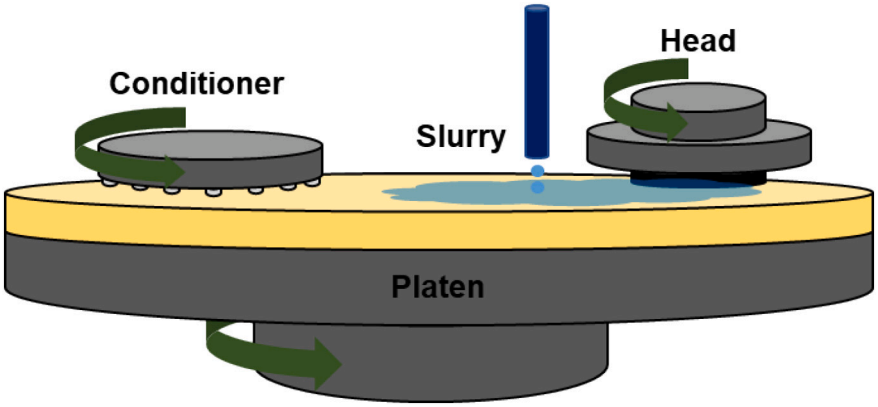

Fig. 1. Schematic of the CMP process.

Table 1
CMP application conditions.

	Conditioning	Polishing
Process time (s)	60	120
Plate speed (rpm)	93	93
Head speed (rpm)	–	87
Head pressure (psi)	–	3
Conditioner pressure (kgf)	3	3
Flow rate (mL/min)	180	180

2. Experimental details

2.1. CMP application and materials

Amorphous carbon was deposited on the Si substrate. A POLI 400 CMP system (GnP Technology) was modified for the experiments to allow simultaneous in situ polishing and conditioning. A standard polyurethane IC-1010 K-groove pad (Dow Chemical Corporation) and conditioner (SAESOL-diamond) using 20PPW60EBC0 diamond grit were used. The test samples were segmented into 4 cm × 4 cm pieces using a dicing diamond cutter. A schematic of the CMP process is shown in Fig. 1, and the conditions are listed in Table 1.

The CMP process involves the disruption of polymer chains using an oxidant additive based on colloidal silica. Additives can be categorized as nonmetal-based oxidants, metal-based oxidants, and electrolytes. Hydrogen peroxide (H_2O_2), potassium nitrate (KNO_3), potassium chloride (KCl), and potassium sulfate (K_2SO_4) were sourced from Sigma-Aldrich. The weight percentages (wt%) of the slurry was calculated for the total solution, and the pH was adjusted using potassium hydroxide (KOH) and nitric acid (HNO_3). The pH meter used was an MCU-710 (KEM Corporation). As the in-situ method used in this study required only minimal amounts of additives, the ions generated during the addition process did not have a significant influence. The removal rate was evaluated after stirring the solution for 12 h using a ball mill, and adding it to the slurry disrupted the dispersion stability. Some of the typical removal rate measurement methods include ellipsometry, reflectometry, and weight loss. However, in this study, the vertical

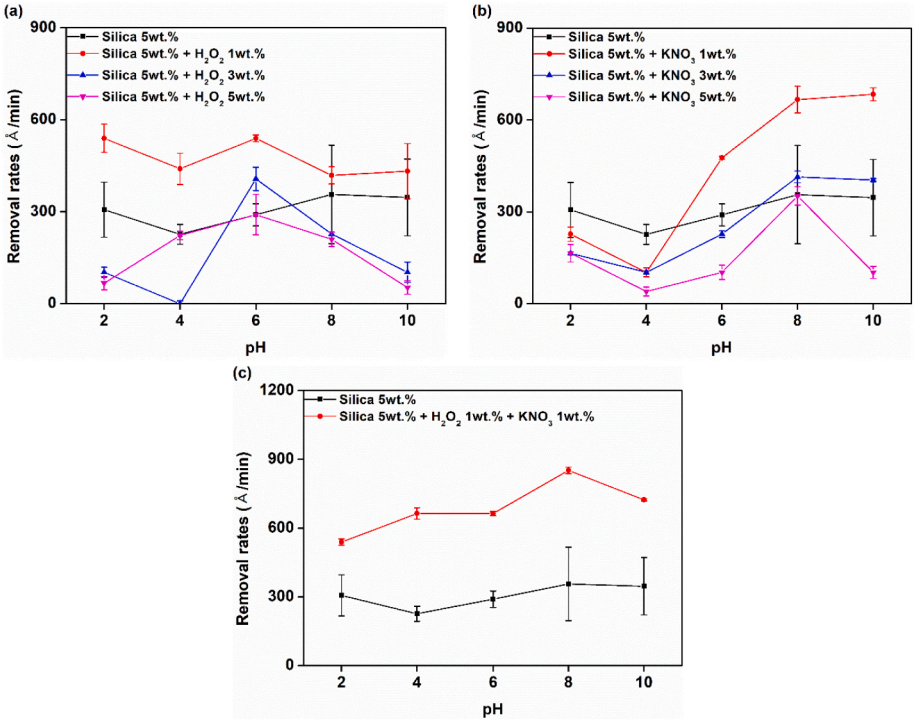

Fig. 2. Removal rates based on a 5 wt% silica slurry containing (a) H_2O_2, (b) KNO_3, and (c) H_2O_2 + KNO_3 in a pH range of 2 to 10.

scanning electron microscopy (SEM) method was used. This unique method was selected because of the thickness of the amorphous carbon layer and the inability of the standard methods to recognize sources without reflectivity. The sample size was fixed to 0.4 × 0.4 cm^2, and the test was carried out in triplicate. The flatness of the wafer surface was measured by atomic force microscopy (AFM), which was carried out in a non-contact mode using a cantilever tip using the Park Systems NX10. An area of 5 μm^2 was scanned around the center of each sample. The mean values of the surface roughness (R_a) and root mean square (R_q) values were calculated using AFM.

2.2. Methods of the analysis

The formation of OH radicals was evaluated by ultraviolet-visible (UV − Vis) spectroscopy by scanning over a wavelength range of 600–300 nm [16,17]. Salicylic acid was added to the slurry at a concentration of approximately 0.04 wt%. Spectroscopic measurements were made on the liquid slurry from the CMP process. X-ray photoelectron spectroscopy (XPS) was used to understand the chemical reaction, and XPS spectra were acquired using an ESCA 2000 instrument (VG Microtech Corporation). The X-ray sources used were twin-anode Al Kα (1486.6 eV) and Mg Kα (1253.6 eV). The scan was recorded at an angle of 56° under a vacuum pressure of 10^{-10} Torr. The sample size was fixed at 1 × 1 cm^2, and survey scans were carried out for C 1 s and O 1 s. Dynamic laser scanning (DLS) and zeta-potential measurements were performed using ELSZ-2000 (Otsuka Co.). Both these measurements are key indicators of the stability of abrasive dispersions. Indirect evidence of agglomeration can be observed in these tests. Each measurement presented herein is the result of an average of five scans. All the tests were performed after cleaning with deionized (DI) water and N_2 gas.

3. Results

3.1. Amorphous carbon removal mechanism

Two types of abrasives are commonly used in the CMP process. The silica abrasive is more effective in the mechanical reaction, whereas the ceria abrasive is more effective in the chemical reaction. Unless the surface induces a chemical effect after the mechanical effects, the amorphous carbon layer is not removed because of the properties of the hard surface and chemical resistance. In fact, the ceria abrasive is not capable of removing the carbon layer. However, silica abrasives are capable of removing the carbon layer with low removal rates. Colloidal silica was used to improve the removal rate. It is known that with an increase in the concentration of process-based nano sized colloidal silica, its removal rate increases [18]. A similar trend was observed when the concentration increased from 1 to 5 wt%. Therefore, the concentration of silica slurry was fixed at 5 wt%. Despite a concentration of 5 wt%, the removal rates were 300 Å/min. Therefore, oxidants were selected for surface oxidation.

Fig. 2 depicts the material removal rates recorded during CMP process of amorphous carbon. The oxidant concentration ranged from 1 wt % to 5 wt%. The removal rates of the H_2O_2 and KNO_3 additive slurries increased owing to oxidation; however, at oxidant concentrations of 3 wt% and 5 wt%, the removal rates decrease, as shown in Fig. 2 (a) and (b). Such a trend of decreased removal rates could be caused by an increase in concentration, thereby resulting in a disturbed CMP process. The rate of removal of the layer was lower that of the oxidant layer, which was disturbed by the passivation layer. Therefore, electrolytes were added to increase the rate of dissociation and prevent the removal rate from decreasing.

As shown in Fig. 2 (c), the removal rates significantly increase (852.21 Å/min) at a pH value of 8. KNO_3 acted as an electrolyte to improve the role of the oxidants in H_2O_2. The electrolyte increased dissolution by increasing the ion strength. All pH values increased the removal rates with the electrolytes. Above all, in the alkaline areas, the removal rates increased. That is because the alkaline area easily forms Si $(OH)_4$ in the silanol groups between the silica abrasive and wafer surface. Increased silanol groups increased the removal rates [19]. The UV–Vis spectroscopy can use to confirm the increase in OH radicals in the silanol groups caused by the electrolytes in the mixed slurry conditions.

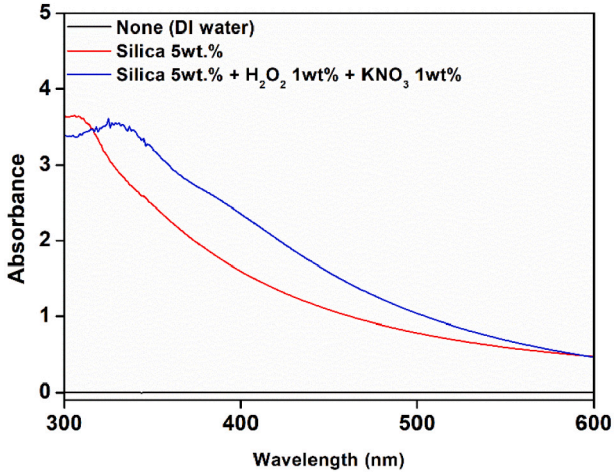

Fig. 3. UV–Vis spectroscopy results of the slurry for the formation of OH radicals. The results indicate the change of 4-hydroxybenzonic acid to 2,3-dihydrobenzoic acid.

In general, colloidal silica processing results in the formation of OH radicals on the surface of silanol groups due to oxidation. The H_2O_2 oxidant generates a significant amount of OH radicals, but due to their inert nature, these radicals are limited to the target material. The addition of the electrolyte, on the other hand, facilitated the formation of OH radicals. UV–Vis spectroscopy demonstrated the resulting increase in the removal rates with an increase in OH radical concentration. As is already known, the wavelength of 4-hydroxybenzonic acid is 300 nm and that of 2,3-dihydrobenzoic acid is 330 nm [17].

Fig. 3 depicts the UV–Vis spectra of the slurry after CMP, 4-hydroxybenzonic acid, and the different additives after 2 min of CMP processing. The results demonstrate that the OH radicals are generated by the oxidants, and the reaction is facilitated by the electrolytes. The results also confirm that 4-hydroxybenzonic acid is converted to 2,3-dihydrobenzoic acid by the addition of an oxidant [17]. For the colloidal silica abrasive, an increase in the amount of OH radicals result in a significant increase in the removal rate. Therefore, it is evident that the

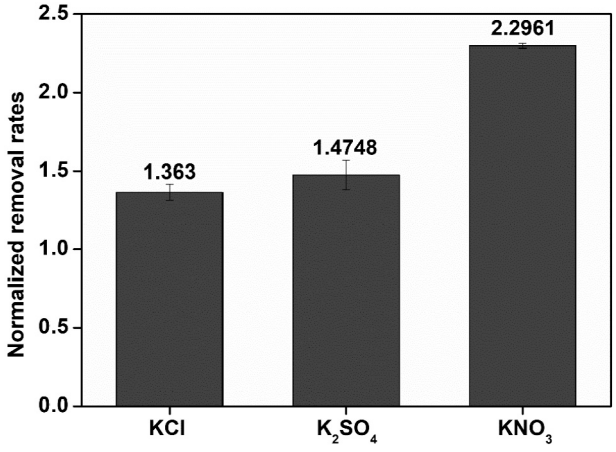

Fig. 4. Effect of K^+ ionic strength on the normalized removal rates. (Normalized removal rates represent the removal rates of the slurry after the addition of electrolytes / the removal rates of a slurry devoid of electrolytes.)

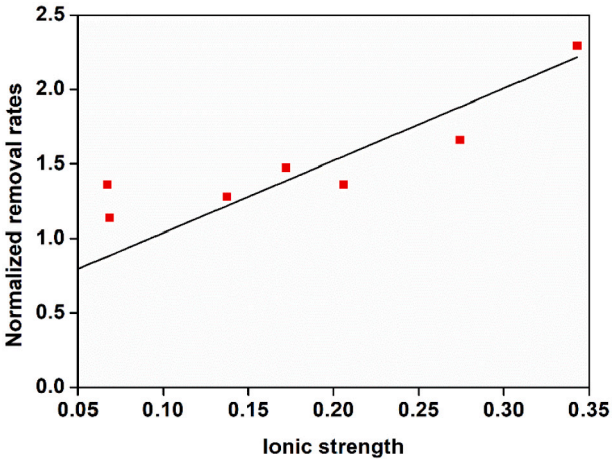

Fig. 5. Regression analysis results of the normalized removal rates with different K^+.

hard and inert target materials in the CMP process require strong oxidants and appropriate additives such as the electrolytes.

3.2. Ionic strength depending on the solution type and concentration

The results confirmed that the electrolyte increased the removal rates by oxidation. The reason for this is ionic strength, which is a measure of the extent of ion dissociation caused by the electrolyte in the solution. Various types of solutions were used to determine the relationship between ionic strength and removal rate. Eq. (1) was used to calculate ionic strengths of various solutions using [20].

$$I = \frac{1}{2}\sum_{i=1}^{n} C_i Z_i^2 \quad (1)$$

(C_i = molar concentration, Z_i = number of ions)The electrolyte solutions used were KNO_3, KCl, and K_2SO_4. The ionic strength of 5 wt% silica +1 wt% H_2O_2-based slurry at a pH value of 8 was quantified. The ionic strengths of the electrolytes, KCl, K_2SO_4, and KNO_3, calculated using the above equation, were 0.067, 0.172, and 0.343 M, respectively (Fig. 4).

The normalized removal rates of KCl, K_2SO_4, and KNO_3 can be calculated by dividing the removal rates of the slurry after the addition of electrolytes by the removal rates of a slurry devoid of electrolytes. The results are as follows: 1.3630, 1.4748, and 2.2961, respectively. The

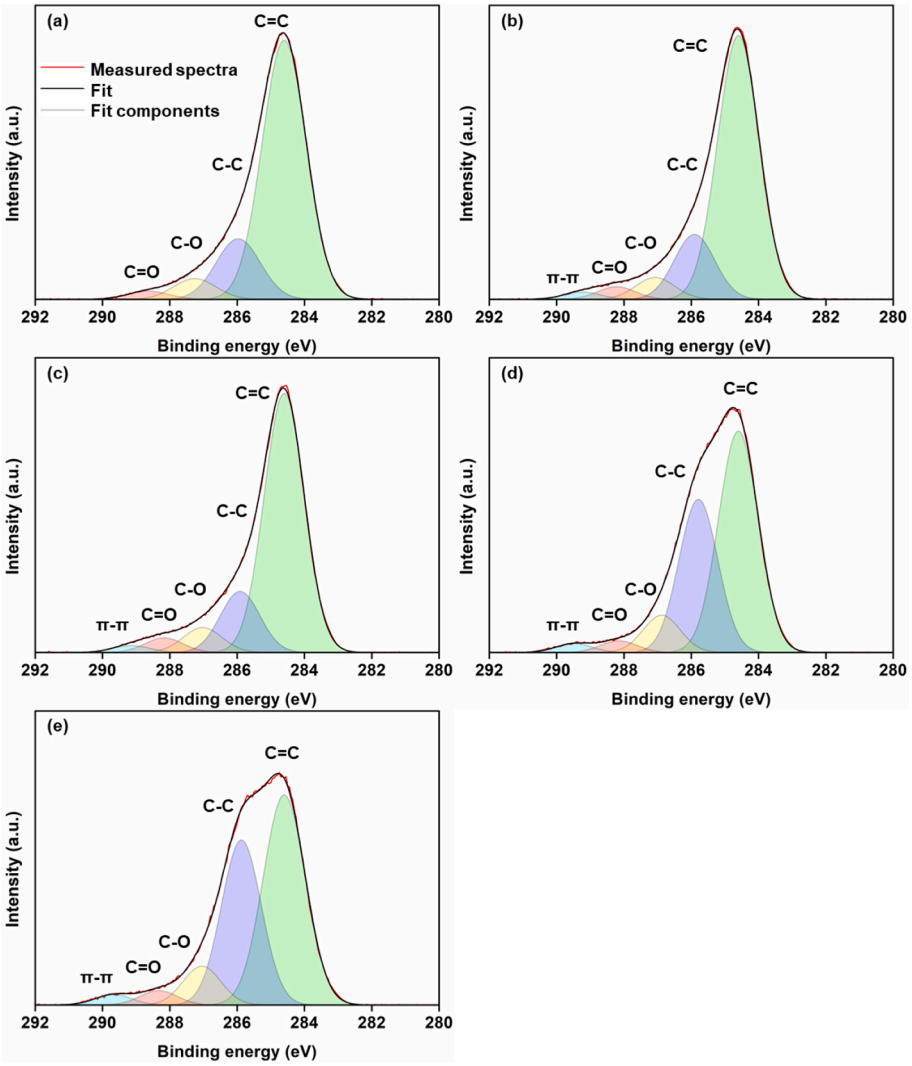

Fig. 6. XPS results after the CMP process for different slurry conditions, (a) C 1s of reference wafer, (b) C 1s of 5 wt% silica, (c) C 1s of 5 wt% silica +1 wt% H_2O_2, (d) C 1s of 5 wt% silica +1 wt% KNO_3, and (e) C 1s of 5 wt% silica +1 wt% H_2O_2 + 1 wt% KNO_3.

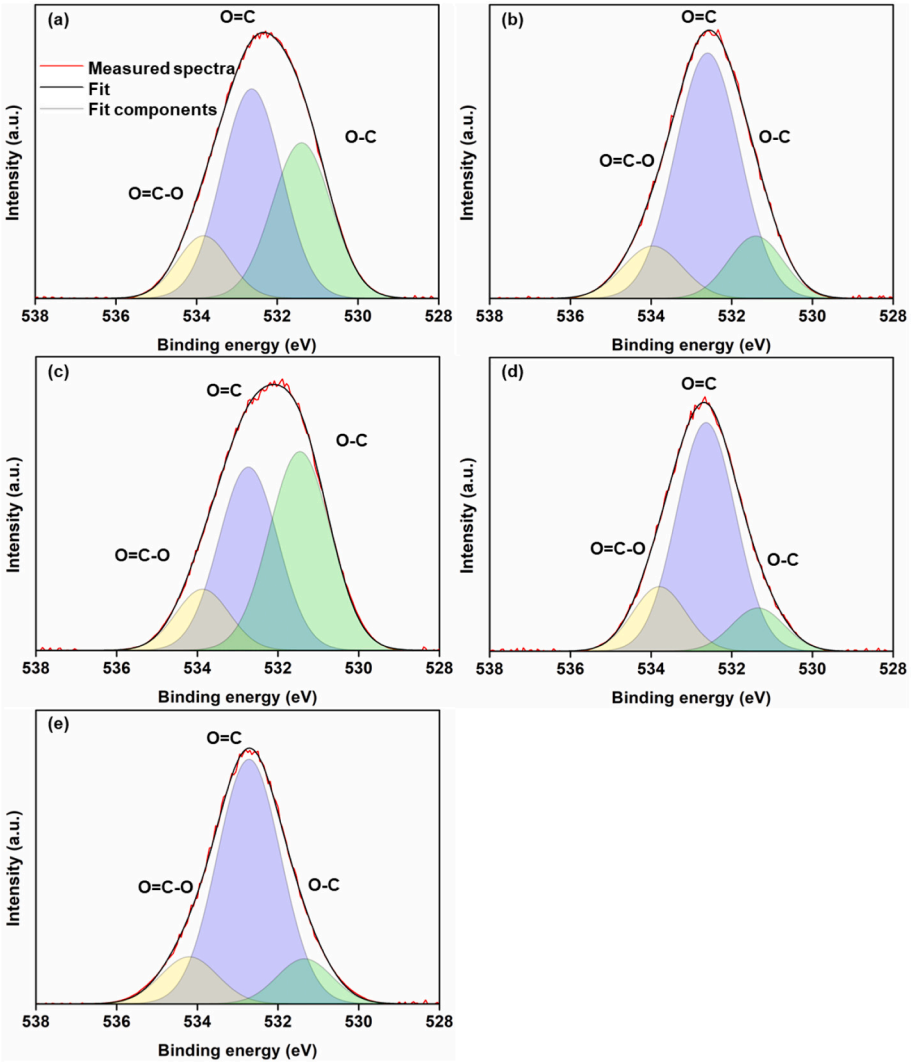

Fig. 7. XPS results after the CMP process for different slurry conditions, (a) O 1s of reference wafer, (b) O 1s of 5 wt% silica, (c) O 1s of 5 wt% silica +1 wt% H_2O_2, (d) O 1s of 5 wt% silica +1 wt% KNO_3, and (e) O 1s of 5 wt% silica +1 wt% H_2O_2 + 1 wt% KNO_3.

removal rates tended to increase with ionic strength. Although different types of electrolytes exhibit different ionic strengths when added to the same quantity of electrolyte, the removal rates were increased by the ionic strength of Eq. (1) and, not by the amount of electrolyte.

The removal rates were confirmed using the ionic strength of the same types of electrolytes. In this study, a KNO_3 additive, high ionic strength, was used. It should be noted that the unit representations of 5 g, 1 wt%, and 0.0098 M all represent the same ion concentration. The experiment was carried out between 1 g (0.0686 M) and 15 g (1.029 M), and the results are shown in Fig. 5. With the addition of the electrolyte, the ionic strength increased, and the removal rate increased to approximately 0.3 mol. However, as concentrations increased, this effect gradually decreased. In addition, a high concentration can cause stability issues, the stability of the slurry was evaluated.

Table 2
XPS results (C 1s peaks) of the amorphous carbon surface at a pH value of 8 and at various slurry conditions.

C1s peaks	C=C	C-C	C-O	C=O	π-π	Total
None	64.51	15.19	4.95	1.88	–	86.53
5 wt% Silica	63.16	15.13	4.91	2.72	1.51	87.43
5 wt% Silica+1 wt% H_2O_2	62.77	14.6	5.85	3.32	1.29	87.83
5 wt% Silica+1 wt% KNO_3	48.05	32.6	7.57	2.34	1.74	92.3
5 wt% Silica+1 wt% H_2O_2 + 1 wt% KNO_3	45.46	33.74	7.52	2.73	1.95	91.4

3.3. Chemical bonding with silica particles and carbon layer

The chemical bonding between the silica abrasive and carbon layer was confirmed using XPS analysis. The C 1 s and O 1s peaks were evaluated using an XPS surface analysis. The amorphous carbon layer primarily consists of carbon and oxides. Therefore, surface analysis was performed to evaluate the C 1s and O 1s peaks. The oxidation mechanism is revealed by the O 1s peaks. The C 1s peaks are divided into five parts, and their assignment follows a typical case for carbon materials as follows: peak 1 at 284.6 eV (C=C), peak 2 at 285.9 eV (C—C), peak 3 at 287.1 eV (C—O), peak 4 at 288.2 eV (C=O), and peak 5 at 289.2 eV(π–π) [21]. Dangling bonds appeared only in the oxidation slurry after CMP. These results indicate that the oxidation process proceeds when the Si—O—C bonds are broken [22,23]. With the addition of the following two oxidants: H_2O_2 and KNO_3, the number of C—O and C=O bonds increased owing to oxidation. When KNO_3 was added, the number of C—C bonds increased remarkably (15.19%–33.74%), whereas that of C=C bonds decreased (64.51%–45.46%) in Fig. 6. Thus, the frequency of carbon single bonding increases as the frequency of carbon double bonding decreases. This is because the C=C bond is converted to a C—C bond via hydration [24].

Table 3
XPS results (O 1s peaks) of the amorphous carbon surface at a pH value of 8 and at various slurry conditions.

O 1s peaks	O-C	O=C	O=C-O	Total
None	4.94	6.78	1.76	13.48
5 wt% Silica	1.81	8.41	1.65	11.88
5 wt% Silica+1 wt% H_2O_2	5.53	4.92	1.49	11.94
5 wt% Silica+1 wt% KNO_3	0.91	5.43	1.37	7.71
5 wt% Silica+1 wt% H_2O_2 + 1 wt% KNO_3	1.03	6.46	1.11	8.6

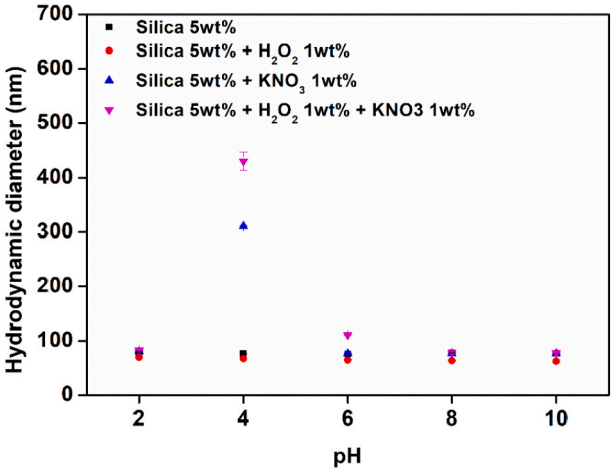

Fig. 8. Effect of pH and different slurry conditions on the hydrodynamic diameter.

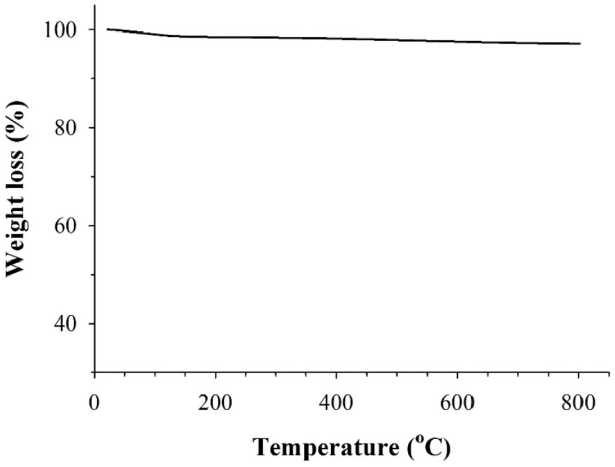

Fig. 9. TGA curves of pristine silica nano particles.

Similarly, the O 1s peaks can be divided into the following three peaks: peak 1 at 530.9 eV (O—C), peak 2 at 532.1 eV (O=C), and peak 3 at 533.4 eV (O=C—O) [21]. The frequencies of O—C and O=C bonding decreased in the H_2O_2 slurry with additives. When KNO_3 was added, a decrease in the number of O—C bonds was observed in the slurry in Fig. 7. Ionic strength was induced by the electrolyte to increase the removal rate. The removal of amorphous carbon resulted in the formation of O—C (1076.38 Kcal / mol) bonds, which induced oxidation on the surface of the carbon film. Furthermore, silica reacted to form Si—O (766.6 kcal/mol) bonds. Therefore, as Si—O—C bonds were formed, C—C (618.3 kcal/mol) bonds with a relatively lower bond strength were broken. This resulted in the surface being polished [24,26,27] (Tables 2 and 3).

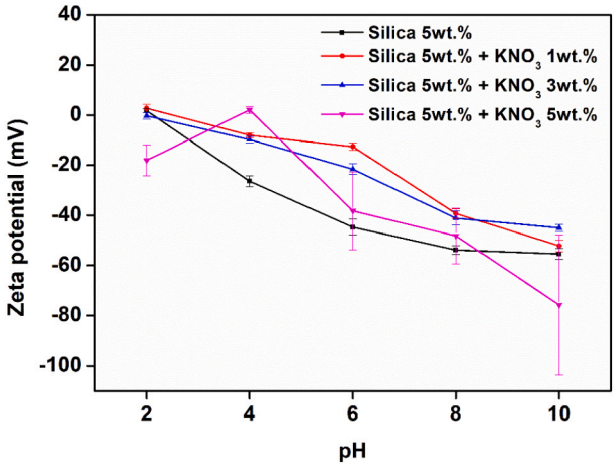

Fig. 10. The zeta potential of colloidal silica with KNO_3 added to DI water over the pH range of 2–10. (Slurries containing H_2O_2 were excluded owing to bubble limitations).

3.4. Stability of the slurry

The particle size for different pH values was confirmed first by using DLS. In general, with an increase in the additive concentration, the unstable dispersion of the abrasive also increases. However, the stability of the particles was maintained as shown in Fig. 8 except a pH values of 2 and 4. Stable dispersion can be induced by the addition of a steric dispersant. Therefore, thermogravimetric analysis (TGA) was performed to confirm the presence of the additives. As shown in Fig. 9, the slurry did not contain any other stabilizing agent because of the tendency of weight loss with increasing temperature [21]. Zeta potential measurements were performed in unstable areas with pH values of 2 and 4, as shown in Fig. 10. The measurement of the zeta potential for H_2O_2 is complicated under our conditions due to bubble formation. The isoelectric point is the pH range between 2 and 4, which means it crosses zero. Particles may agglomerate within this unstable region, increasing their size. This why the particle size was large, as shown in Fig. 8. The overall zeta potential increased when the electrolyte was added. The addition of KNO_3 increased the zeta potential, which can be explained by the ionic strength [15]. However, a similar trend was not observed with the 5 wt% additive owing to the excessive addition of electrolytes as indicated by the standard deviation. The excess additive results in aggregation and agglomeration despite the stable region of zeta potential. Although the electrolyte helps to stabilize the dispersion, the condition of the slurry with excess additive needs to be avoided.

3.5. Flatness after amorphous carbon CMP

The roughness of the surface after polishing is as important as the removal rate, and can affect further processes. R_a and R_q values were calculated to evaluate roughness [29]. An image of the amorphous carbon surface before CMP is shown in Fig. 11 (a), where the values of R_a and R_q are 1.454 and 1.858 nm, respectively. Fig. 11 (b) shows the values of R_a and R_q change to 1.096 and 1.411 nm, respectively when the abrasive is added. Fig. 11 (c) shows that the values of R_a and R_q are 1.288 and 1.616 nm, respectively for the non-metal-based oxidant H_2O_2 while for the metal-based oxidant KNO_3 in Fig. 11 (d), the values of R_a and R_q are 0.26 nm and 0.367 nm, respectively. Fig. 11 (e) shows the R_a and R_q are 0.147 and 0.264, respectively for the mixed slurry. Therefore, in all cases, an improvement in the roughness value was observed; the mixed slurry exhibited the highest improvement in roughness value of approximately 0.147 nm. Furthermore, organic residues or particles were still found on the surfaces of all specimens, and the residues had to be removed prior to further processing. As a result, further research on

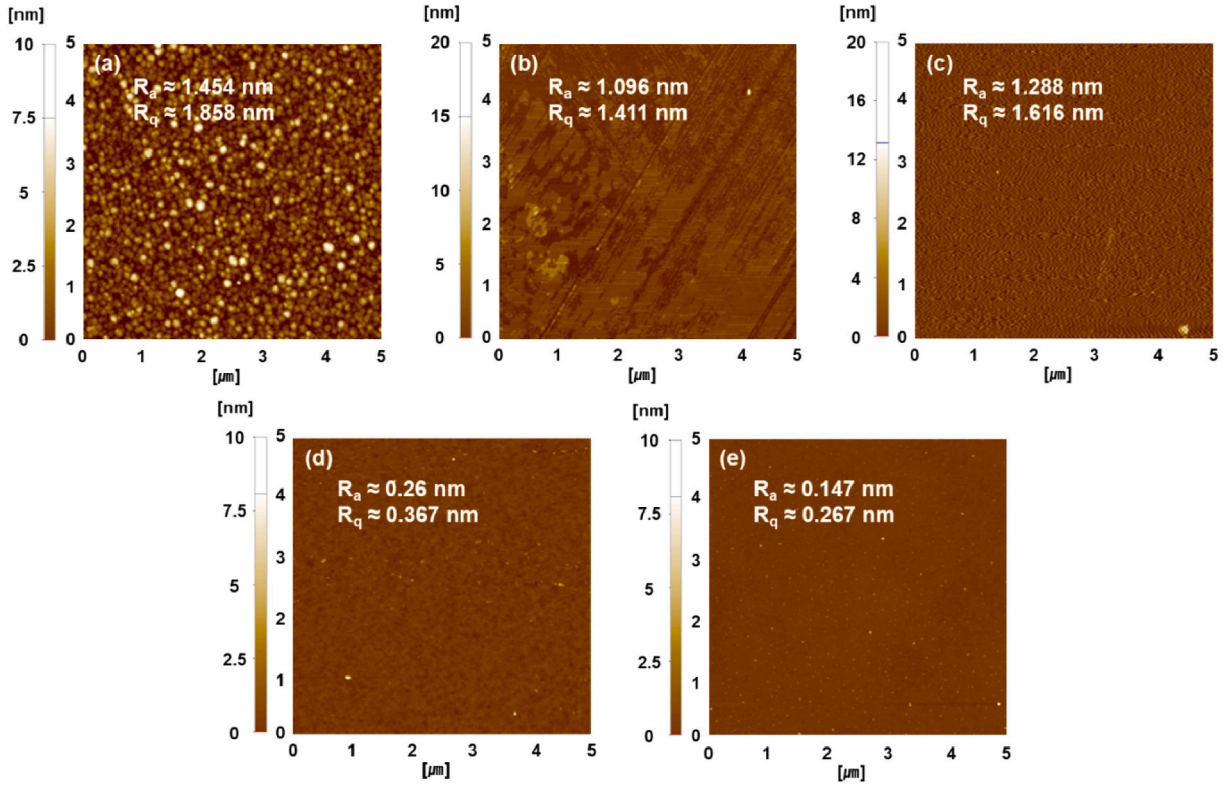

Fig. 11. AFM images of the amorphous carbon surface: (a) reference wafer, (b) 5 wt% silica, (c) 5 wt% silica +1 wt% H_2O_2, (d) 5 wt% silica +1 wt% KNO_3, and (e) 5 wt% silica +1 wt% H_2O_2 + 1 wt% KNO_3.

post-CMP cleaning.

4. Conclusion

The amorphous carbon CMP process involves oxidation to disrupt polymer chains. Mechanical and chemical reactions eliminated the oxidation layers. Ionic strength was used in this study to increase the removal rate by adding electrolytes. The added electrolyte aids the dissolution and stabilization of the dispersion phenomenon. During removal, Si—O—C—C and Si—O—C=C bonds were formed by chemical reactions, and some of these bonding-like aggregates were eliminated by shear forces. The C—C bonds were less stable than the C=C bonds due to their lower bonding strength. Furthermore, as the CMP process progressed locally at high temperatures the C=C bonds were converted to C—C bonds by carbon hydrogenation. When the electrolyte was added to the slurry, the removal reaction reacted more strongly with the ionic strength. Therefore, it can be concluded that electrolytes can be used to achieve higher removal rates and better roughness values. This study presents an overall mechanism for using amorphous carbon to measure ionic strength. However, further research is required to fully understand this mechanism.

CRediT authorship contribution statement

Seungjun Oh Conceptualization, Writing - Original Draft, Writing- Reviewing and Editing, Methodology, Investigation

Cheolmin Shin Conceptualization, Writing - Original Draft, Writing- Reviewing and Editing, Methodology, Investigation

Donggeon Kwak Validation, Formal analysis

Eungchul Kim Validation, Visualization

Juhwan Kim Validation, Visualization

Chulwoo Bae Resources, Investigation.

Taesung Kim Supervision, Writing- Reviewing and Editing, Project administration

Declaration of competing interest

The authors declare that they have no known competing financial interests or personal relationships that could have appeared to influence the work reported in this paper.

References

[1] S. Pauliac-Vaujour, P. Brianceau, C. Comboroure, O. Faynot, Improvement of high resolution lithography by using amorphous carbon hard mask, Microelectronic Engineering 85 (2008) 800–804.
[2] F. Awaja, T.-T. Wong, D. Putzer, M. Thaler, A. al Taee, T. O'Brien, Molecular descriptions of functionalised multi layered diamond like/ amorphous carbon coatings, Materials Today Communications 19 (2019) 433–440.
[3] J. Robertson, Diamond-like amorphous carbon, Mater. Sci. Eng. R. Rep. 37 (2002) 129–281.
[4] R. Pandiyan, N. Delegan, A. Dirany, P. Drogui, M.A. El Khakani, Correlation of sp2 carbon bonds content in magnetron-sputtered amorphous carbon films to their electrochemical h2o2 production for water decontamination applications, Carbon 94 (2015) 988–995.
[5] Zhenyu Zhang, et al., Environment friendly chemical mechanical polishing of copper, Applied Surface Science 467 (2019) 5–11.
[6] Zhenyu Zhang, et al., Chemical mechanical polishing for sapphire wafers using a developed slurry, Journal of Manufacturing Processes 62 (2021) 762–771.
[7] Zhenyu Zhang, et al., Development of a novel chemical mechanical polishing slurry and its polishing mechanisms on a nickel alloy, Applied Surface Science 506 (2020), 144670.
[8] Longxing Liao, et al., A novel slurry for chemical mechanical polishing of single crystal diamond, Applied Surface Science 564 (2021), 150431.
[9] Wenxiang Xie, et al., Green chemical mechanical polishing of sapphire wafers using a novel slurry, Nanoscale 12 (44) (2020) 22518–22526.
[10] T. Du, D. Tamboli, V. Desai, S. Seal, Mechanism of copper removal during cmp in acidic h2o2 slurry, J. Electrochem. Soc. 151 (2004) G230–G235.
[11] L. Jiang, Y. He, Y. Li, J. Luo, Effect of ionic strength on ruthenium cmp in h2o2-based slurries, Appl. Surf. Sci. 317 (2014) 332–337.
[12] W. Choi, U. Mahajan, S.-M. Lee, J. Abiade, R.K. Singh, Effect of slurry ionic salts at dielectric silica cmp, J. Electrochem. Soc. 151 (2004) G185–G189.
[13] G.B. Basim, I.U. Vakarelski, B.M. Moudgil, Role of interaction forces in controlling the stability and polishing performance of cmp slurries, J. Colloid Interface Sci. 263 (2003) 506–515.

[14] J. Matovu, N. Penta, S. Peddeti, S. Babu, Chemical mechanical polishing of ge in hydrogen peroxide-based silica slurries: role of ionic strength, J. Electrochem. Soc. 158 (2011) H1152–H1160.
[15] U.R.K. Lagudu, S. Isono, S. Krishnan, S.V. Babu, Role of ionic strength in chemical mechanical polishing of silicon carbide using silica slurries, Colloids Surf. A Physicochem. Eng. Asp. 445 (2014) 119–127.
[16] Y. Zhou, G. Pan, X. Shi, H. Gong, G. Luo, Z. Gu, Chemical mechanical planarization (cmp) of on-axis si-face sic wafer using catalyst nanoparticles in slurry, Surf. Coat. Technol. 251 (2014) 48–55.
[17] D. Minakata, W. Song, S.P. Mezyk, W.J. Cooper, Experimental and theoretical studies on aqueous-phase reactivity of hydroxyl radicals with multiple carboxylated and hydroxylated benzene compounds, Phys. Chem. Chem. Phys. 17 (2015) 11796–11812.
[18] D. Tamboli, G. Banerjee, M. Waddell, Novel interpretations of cmp removal rate dependencies on slurry particle size and concentration, Electrochem. Solid-State Lett. 7 (2004) F62–F65.
[19] Uma R.K. Lagudu, et al., Reactive liquids for non–prestonian chemical mechanical polishing of polysilicon films, ECS Journal of Solid State Science and Technology 8.5 (2019), P3040.
[20] A.D. McNaught, Compendium of Chemical Terminology, Blackwell Science Oxford, 1997.
[21] C.-C. Teng, C.-C.M. Ma, C.-H. Lu, S.-Y. Yang, S.-H. Lee, M.-C. Hsiao, M.-Y. Yen, K.-C. Chiou, T.-M. Lee, Thermal conductivity and structure of non-covalent functionalized graphene/epoxy composites, Carbon 49 (2011) 5107–5116.
[22] E.L.H. Thomas, G.W. Nelson, S. Mandal, J.S. Foord, O.A. Williams, Chemical mechanical polishing of thin film diamond, Carbon 68 (2014) 473–479.
[23] G. Chen, Z. Ni, Y. Bai, Q. Li, Y. Zhao, The role of interactions between abrasive particles and the substrate surface in chemical-mechanical planarization of si-face 6h-sic, RSC Adv. 7 (2017) 16938–16952.
[24] A.W. Johnson, Invitation to Organic Chemistry, Jones & Bartlett Learning, 1999.
[26] A. Peguiron, G. Moras, M. Walter, H. Uetsuka, L. Pastewka, M. Moseler, Activation and mechanochemical breaking of c–c bonds initiate wear of diamond (110) surfaces in contact with silica, Carbon 98 (2016) 474–483.
[27] Y.-R. Luo, Handbook of Bond Dissociation Energies in Organic Compounds, CRC press, 2002.
[29] B.R. Kumar, T.S. Rao, Afm studies on surface morphology, topography and texture of nanostructured zinc aluminum oxide thin films, Digest Journal of Nanomaterials and Biostructures 7 (2012) 1881–1889.